Two-Dimensional Supramolecular Assemblies of a Polydiacetylene. 1. Synthesis, Structure, and Third-Order Nonlinear Optical Properties

K. E. Huggins,† S. Son,† and S. I. Stupp*,†,‡

Departments of Materials Science and Engineering and Chemistry, Materials Research Laboratory, Beckman Institute for Advanced Science and Technology, University of Illinois at Urbana-Champaign, Urbana, Illinois 61801

Received November 21, 1996; Revised Manuscript Received June 4, 1997⊗

ABSTRACT: A diacetylene monomer with a rigid backbone and capable of forming hydrogen bonds was synthesized and found to polymerize forming two-dimensional supramolecular assemblies. The two-dimensional structure self-assembles when UV light generates polydiacetylene comb polymers, and hydrogen bonds are established within molecular layers. The two-dimensional assemblies have been characterized by X-ray diffraction and infrared spectroscopy and found to consist of highly ordered bilayers. The material forms blue solid thin films which generate third-order nonlinear optical signals and have remarkable photochemical stability to 1064 nm radiation from a Q-switched Nd:YAG laser. Upon heating to 62 °C, the material turns bright red reversibly while maintaining its two-dimensional structure, and this thermochromic process is accompanied by endothermic and exothermic signatures detected by differential scanning calorimetry. Most importantly, however, variable temperature sum frequency generation experiments show that the third-harmonic generation signals retain much of their original intensity through the thermochromic transitions. These results do not conform in a consistent manner to both the theory of third-order effects and the previously suggested connection between intramolecular conjugation and optical absorption of polydiacetylenes. It is therefore possible that intermolecular interactions in these highly ordered structures play a role in defining optical properties.

Introduction

Most of polymer science has studied one-dimensional linear chains and three-dimensional gels. It is interesting to fill in the "dimensionality gap" between linear polymers and cross-linked networks and explore the consequences on physical properties. Discrete two-dimensional polymers and two-dimensional supramolecular assemblies are part of this gap. Previous work investigated two-dimensional (2D) molecular systems such as Langmuir−Blodgett (LB) films,[1,2] self-assembled monolayers,[3−5] and infinite 2D networks formed at oil−water interfaces[6] and within amphiphilic bilayers.[7,8] Many of these systems are not truly self-assembling given the requirement of external boundaries to drive their formation. However, we reported recently on 2D polymers which form in bulk by self-assembly because 2D organization for the required chemical reactions is encoded in the precursor molecules. In the first systems we demonstrated that temporal relaxation of second-harmonic generation activity does not occur in macroscopic films composed of these 2D polymers.[9] Since molecular alignment is not as critical in third-order systems many different types of molecular architectures are available to study third-order effects. In addition to crystals,[10,11] linear, branched, and ladder polymers[17−21] have been investigated for their third-order nonlinear optical properties. It is of great interest to pursue how new architectures such as two-dimensional materials affect the third-order nonlinear optical properties. Here we report on self-assembling two-dimensional supramolecular assemblies formed by comb polymers and their third-harmonic generation properties.

The system studied here takes advantage of the directionality and reactivity of topochemical polymerizations in crystalline solids. It is well known that these reactions are greatly influenced by the way molecules pack in the solid state.[22−26] Since diffusion of monomer within the solid is effectively forbidden, the lattice structure of the precursor dictates the reactivity. As schematically illustrated in Figure 1, if monomers contain at least two polymerizable groups that are well aligned in separate planes with at least one group located away from molecular termini, then two possible macromolecular architectures may emerge. "Parallel" polymerization occurs in both planes, and ladder poly-

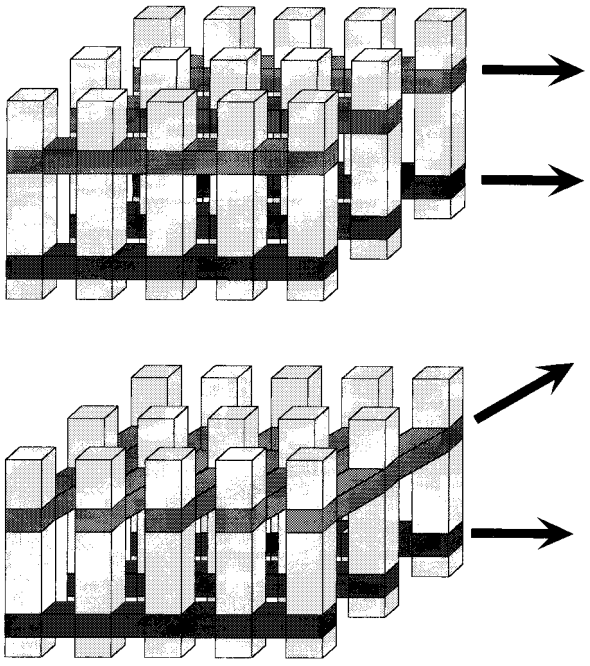

Figure 1. Top: Schematic representation of a precursor containing two polymerizable groups forming ladders via "parallel" polymerization. Bottom: Perpendicular polymerization of the same precursor molecules results in a 2D polymer.

* To whom correspondence should be addressed.
† Department of Materials Science and Engineering.
‡ Department of Chemistry.
⊗ Abstract published in *Advance ACS Abstracts,* July 15, 1997.

S0024-9297(96)01715-9 CCC: $14.00

Scheme 1

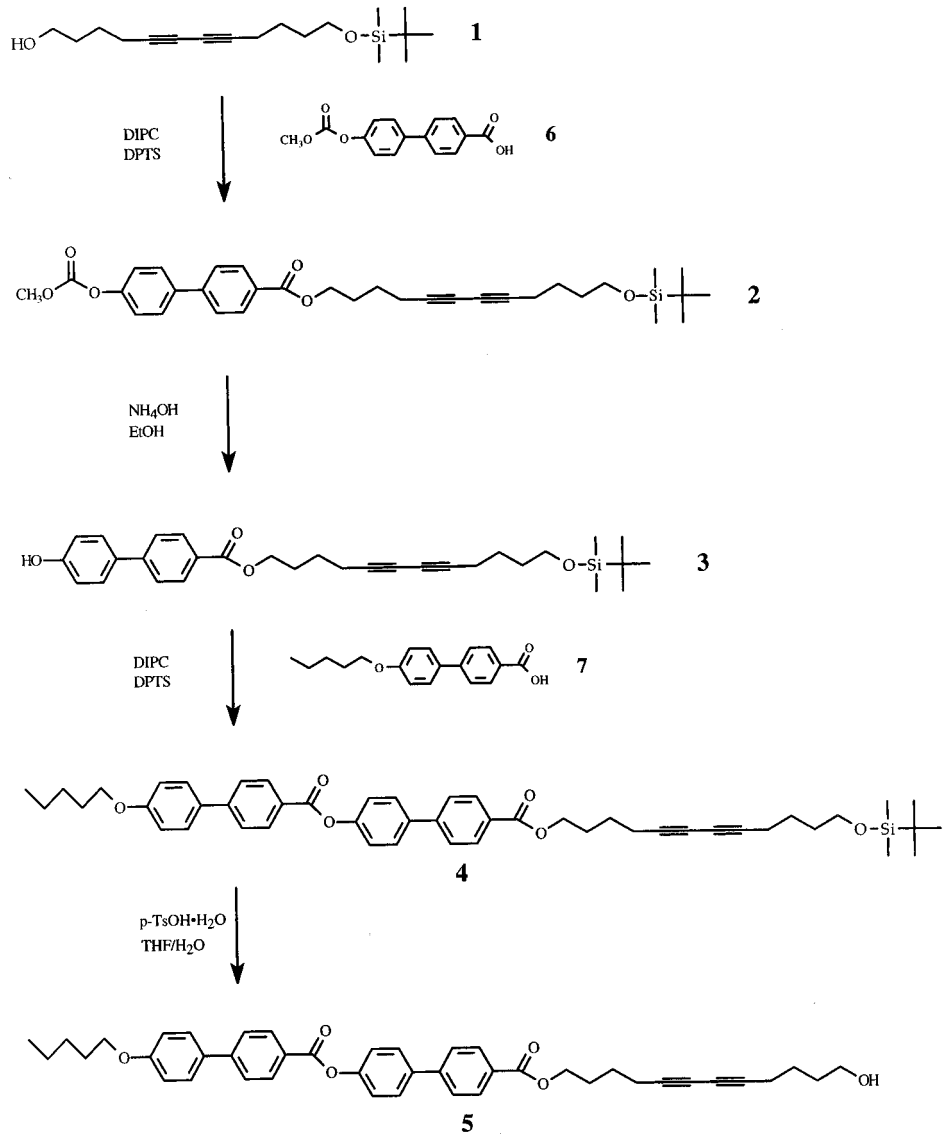

mers form. Alternatively, "perpendicular" polymerizations occur in both planes, and a 2D polymer forms. Decorrelation of the direction of polymerization in the two different reactive planes also results in the formation of a 2D polymer. In our earlier work[27] we pointed out that spatial proximity between the reactive planes raises the probability of forming one-dimensional ladder polymers rather than 2D polymers. In fact, a continuum of architectures should be possible as correlation is gradually lost, producing what we like to call "ladderoid" structures. The structures should become two-dimensional when all correlation is lost.

Polydiacetylenes substituted with various side chains have been studied previously, including some containing hydrogen-bonding groups in the side chain but away from the terminus.[25,28,29] However, none of these materials appear to have the correct structure to form two-dimensional polymers stitched by a combination of covalent and hydrogen bonds. In one system[25] the hydrogen-bonding groups located at the side chain terminus form dimeric hydrogen bonds, and thus the structure does not acquire two-dimensionality. In this work we have synthesized a diacetylene precursor which has the potential to self-assemble into a 2D polymer formed by both covalent bonds (the polydiacetylene backbone) and hydrogen bonds (formed among side chains). We have characterized its structure by X-ray diffraction, infrared spectroscopy, and differential scanning calorimetry. We have also studied its thermochromic transitions and third harmonic generation in an effort to probe the effect of two−dimensionality on structure-property relations.

Experimental Section

Synthesis and Sample Preparation. Monomeric precursor **5** was synthesized in our laboratory, and its preparation is described in Scheme 1 and explained in detail below. Experimental samples were prepared dissolving **5** in a 1:1 mixture of dichloromethane and toluene and casting films approximately 1 cm^2 in area onto glass, quartz, copper, single-crystal silicon, and sapphire substrates. The dried monomer was exposed to 1.5 mW/cm^2 ultraviolet light from a mercury penlamp (peak = 254 nm) for approximately 1 min.

All starting materials were commercially obtained and used without further purification unless otherwise noted. The ^1H NMR spectra were recorded on a General Electric QE-300 instrument at 300 MHz. The catalyst 4-(dimethylamino)-pyridinium 4-toluenesulfonate (DPTS) was synthesized according to the procedure described by Moore and Stupp.[30]

12-[(*tert*-Butyldimethylsilyl)oxy]-5,7-dodecadiyn-1-ol (1). 5,7-Dodecadiyne-1,12-diol (4 g, 20.6 mmol) and imidazole (2.8 g, 41.1 mmol) were dissolved in dimethylformamide (DMF) (15 mL). To the solution was added *tert*-butyldimethylsilyl

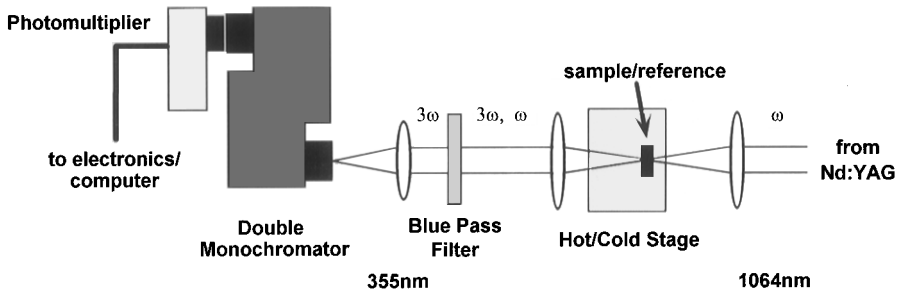

Figure 2. Nonlinear optical experimental setup showing a simplified scheme of the sum frequency experiment.

chloride (2.83 g, 18.8 mmol) all at once. The solution was stirred for 20 h at room temperature under a nitrogen atmosphere. At this point, the reaction mixture was transferred into a separatory funnel along with dichloromethane (100 mL) and washed with saturated sodium bicarbonate solution and water successively. The organic layer was dried ($MgSO_4$) and concentrated followed by purification of the residue by flash chromatography (silica gel, 7% acetone in dichloromethane) affording a pale yellow oil of **1** (3.17 g, yield 55%): ^{1}H NMR (300 MHz, $CDCl_3$) δ 0.04 (s, 6H), 0.88 (s, 9H), 1.5−1.8 (m, 8H), 2.2−2.4 (m, 4H), 3.6−3.8 (m, 4H); MW 308.53 ($C_{18}H_{32}O_2Si$).

4′-[[[12-[(*tert*-Butyldimethylsilyl)oxy]-5,7-dodecadiynyl]-oxy]carbonyl][1,1′-biphenyl] 4-Methoxycarbonate (2). 6 (1.33 g, 4.89 mmol) and DPTS (0.477 g, 1.62 mmol) were suspended in dichloromethane (60 mL). To the solution added was diisopropylcarbodiimide (DIPC) (1.52 mL, 9.72 mmol) followed by addition of **1** (1.5 g, 4.86 mmol) which was diluted in dichloromethane (3 mL). After stirring for 12 h at room temperature under a nitrogen atmosphere, the contents were poured into a separatory funnel, washed with water, dried ($MgSO_4$), and concentrated. The crude intermediate **2** was purified by flash chromatography (silica gel, dichloromethane) and concentrated.

12-[(*tert*-Butyldimethylsilyl)oxy]-5,7-dodecadiynyl 4′-Hydroxy [1,1′-biphenyl]-4-carboxylate (3). 2 was diluted with dichloromethane (20 mL), and a mixture of ammonium hydroxide (29% aqueous solution, 15 mL) and ethanol (50 mL) was added. After stirring for 2.5 h, the solution was washed with saturated sodium bicarbonate and neutralized with hydrochloric acid (1 N). The product was then extracted with dichloromethane, dried ($MgSO_4$), and concentrated to afford a white solid product **3** (1.9 g, yield 77.5%): ^{1}H NMR δ 0.04 (s, 6H), 0.88 (s, 9H), 1.6−2.0 (m, 8H), 2.3−2.5 (m, 4H), 3.62 (t, J = 5.80 Hz, 2H), 4.35 (t, J = 6.37 Hz, 2H), 6.94 (d, J = 8.67 Hz, 2H), 7.53 (d, J = 7.63 Hz, 2H), 7.61 (d, J = 8.73 Hz, 2H), 8.08 (d, J = 8.62 Hz, 2H); MW 504.75 ($C_{31}H_{40}O_4Si$).

4′-[[[12-[(*tert*-Butyldimethylsilyl)oxy]-5,7-dodecadiynyl]-oxy]carbonyl] [1,1′-biphenyl]-4-yl 4′-(*n*-Pentyloxy)[1,1′-biphenyl]-4-carboxylate (4). 3 (310 mg, 1.09 mmol), **7** (500 mg, 0.99 mmol), and DPTS (128 mg, 0.435 mmol) were suspended in chloroform (10 mL) at room temperature under a nitrogen atmosphere. To the solution was added DIPC (0.256 mL, 1.63 mmol) all at once via syringe. After the reaction mixture stirred for 20 h, solid precipitation was removed by vacuum filtration. The solution was then dried ($MgSO_4$) and concentrated. The residue was purified by flash chromatography (silica gel, 33% petroleum ether in dichloromethane) to give a white solid product **4** (3.05 g, yield 80%): ^{1}H NMR (300 MHz, $CDCl_3$) δ 0.042 (s, 6H), 0.89 (s, 9H), 0.95 (t, J = 7.01 Hz, 3H), 1.3−2.0 (m, 14H), 2.2−2.3 (m, 2H), 2.37 (t, J = 6.9 Hz, 2H), 3.62 (t, J = 5.59 Hz, 2H), 4.03 (t, J = 6.57 Hz, 2H), 4.37 (t, J = 6.21 Hz, 2H), 7.01 (d, J = 8.65 Hz, 2H), 7.35 (d, J = 8.46 Hz, 2H), 7.61 (d, J = 8.62 Hz, 2H), 7.6−7.7 (m, 6H), 8.12 (d, J = 8.20 Hz, 2H), 8.26 (d, J = 8.33 Hz, 2H); MW 771.09 ($C_{49}H_{58}O_6Si$).

4′-[[(12-Hydroxy-5,7-dodecadiynyl)oxy]carbonyl][1,1′-biphenyl]-4-yl 4′-(*n*-Pentyloxy)[1,1′-biphenyl]-4-carboxylate (5). To a solution of **4** (0.4 g, 0.519 mmol), tetrahydrofuran (THF) (6 mL), and water (0.28 mL) was added *p*-toluenesulfonic acid monohydrate (28 mg, 0.147 mmol) all at once at room temperature. After stirring for 20 h the contents were transferred into a separatory funnel along with dichloromethane (20 mL). The organic layer was washed with water, dried ($MgSO_4$), and concentrated. The crude product was purified by flash chromatography (silica gel, 5% acetone in dichloromethane) affording **5** (0.280 g, yield 82%): ^{1}H NMR (300 MHz, DMSO-d_6) δ 0.87 (t, J = 6.82 Hz, 3H), 1.3−2.0 (m, 14H), 2.0−2.1 (m, 2H), 2.29 (t, J = 6.74 Hz, 2H), 3.80 (t, J = 6.87 Hz, 2H), 3.94 (t, J = 6.49 Hz, 2H), 4.27 (t, J = 6.39 Hz, 2H), 6.93 (d, J = 8.51 Hz, 2H), 7.28 (t, J = 8.49 Hz, 2H), 7.56 (d, J = 8.37 Hz, 2H), 7.6−7.7 (m, 6H), 8.01 (d, J = 8.23 Hz, 2H), 8.14 (d, J = 8.30 Hz, 2H); MW 656.83 ($C_{43}H_{44}O_6$).

4′-[(Methoxycarbonyl)oxy]-4-biphenylcarboxylic Acid (6). 4′-Hydroxy-4-biphenylcarboxylic acid (4 g, 18.67 mmol) and sodium hydroxide (1.64 g, 41.1 mmol) were dissolved in water (50 mL) and ethanol (8 mL) at −10 °C. Methyl chloroformate (1.73 mL, 22.4 mmol) was added to the solution which was maintained at −5 °C. The solution was stirred for 40 min, and a mixture of water and hydrochloric acid (1:1) was added until the solution became acidic. The solid precipitate was collected by vacuum filtration, washed several times with distilled water, and dried, producing **6** (4.72 g, yield 95.5%): ^{1}H NMR (300 MHz, DMSO) δ 3.842 (s, 3H), 7.36 (d, J = 8.68 Hz, 2H), 7.78 (d, J = 8.70 Hz, 2H), 7.80 (d, J = 8.44 Hz, 2H), 8.03 (d, J = 8.65 Hz, 2H); MW 272.25 ($C_{15}H_{12}O_5$).

4-Pentoxybiphenylcarboxylic Acid (7). Synthesis is described in Gray et al.[31]

Characterization. Wide angle X-ray diffraction was carried out using 1.541Å Cu Kα wavelength in a Rigaku/D-Max B powder diffractometer with a graphite monochromator. UV-exposed samples cast on copper substrates were mounted on a hot/cold stage to vary the temperature during X-ray measurements from 0 to 150 °C with an accuracy of ±2 °C. Fourier transform infrared spectroscopy (FTIR) spectra were obtained in a Nicolet IR-30 spectrometer. In one experiment, a monomer solution was cast onto a glass substrate and UV exposed, and the material obtained was ground to prepare KBr pellets for FTIR analysis. In a different experiment, 1 μm thin films were cast onto a 1 mm thick single-crystal silicon substrate (cleaned in a 10% HF solution) and UV exposed. The samples were mounted onto a hot stage and rotated approximately 55° from normal incidence from the transmitted IR beam. This was done in order to minimize noise from internal reflections of the IR beam within the silicon substrate. Absorption spectra from 4800 to 980 cm^{-1} were obtained at 25 °C intervals within the temperature range 25−200 °C. Ultraviolet−visible−near infrared spectra were obtained with a Varian Cary 2200 UV−vis−near infrared spectrophotometer. Variable temperature measurements were carried out by mounting the sample and a plain glass reference onto a hot stage, and absorption spectra were taken from 320 to 900 nm with a line width of 1 nm and obtained at 25 °C intervals from 25 to 200 °C. Differential scanning calorimetry utilized a TA Instruments MDSC 2920 instrument and samples of 5.8−6.0 mg. The samples were heated at 10 °C/min from 0 to 80 °C, held for 2 min at 80 °C, cooled to 0 °C, reheated to 150 °C, held at this temperature for 2 min, and then cooled to 50 °C at 10 °C/min. Other samples were heated from 0 to 250 °C, held at 250 °C for 2 min, and cooled to 50 °C at 10 °C/min.

Nonlinear Optics. A schematic of the third-order sum frequency generation experimental setup is shown in Figure 2. The 1064 nm fundamental for the nonlinear optics experiment was produced by a Molectron MY34-20 Q-switched Nd:

YAG laser with a 20 ns pulse width operating at a 20 Hz repetition rate. Samples were prepared by casting the monomeric precursor onto 1 mm thick single crystal sapphire substrates followed by UV exposure. Sapphire substrates rather than plain glass slides were used to improve thermal conductivity. The sample was mounted onto a hot/cold stage, and data were obtained at 10 °C intervals from 20 to 200 °C. The 1064 nm fundamental was tightly focused onto the sample over a circular area of approximately 150 μm diameter, yielding a peak intensity of 28 MW/cm^2. The third harmonic at 354 nm was separated from the fundamental via a series of blue pass filters and an Instruments SA, Inc. DH-10 double monochromator. The light was collected in a Hamamatsu R1477 photomultiplier tube, and the signal was sent out to a digital data acquisition system and an oscilloscope. A 9 mm thick plain BK7/A substrate obtained from Newport Corp. served as a reference, with $\chi_{ref}^{(3)}(-3\omega;\omega,\omega,\omega) = 0.635 \times 10^{-14}$ esu.[53] All data were corrected for absorption of the 354 nm third harmonic as a function of temperature.

Results and Discussion

Diacetylene monomer **5** was a birefringent white solid, and immediately upon exposure to UV light the compound turned deep blue to the eye and became insoluble but remained birefringent. The blue color is an indication of diacetylene polymerization as typically observed in other systems.[4,5,33−36] The polymerization of diacetylene bonds in **5** has been confirmed and followed with Raman spectroscopy in our laboratory, and these results are reported elsewhere.[37] We observed both solvatochromic and thermochromic color changes in the polymerized deep blue material. A strong solvatochromic effect was observed upon immersion of the polymerized material in dichloromethane or chloroform for approximately 5 min. The blue solid turns to a deep rust-red color which persists for many weeks after removal from the organic liquid, never quite recovering its original blue color. It is likely that this effect is caused by solvent which becomes kinetically trapped within the solid, although its precise location in the structure remains unknown. However, immersing the blue solid into toluene, acetone, or water for many weeks produces no noticeable solvatochromic changes visible to the eye. This is to be expected since the monomer is insoluble in acetone and water and is only weakly soluble in toluene. Application of heat to the polymerized material results in a reversible thermochromic change from blue to bright red above 62 °C. As the temperature is increased further, the polymer irreversibly and gradually changes color from bright red to orange between 110 and 150 °C while maintaining its birefringence. Further application of heat results in a gradual color change to yellow around 200 °C accompanied by a decrease in chromic intensity. Upon cooling to room temperature the polymeric sample acquires and maintains a yellow-orange color. All of the characterization experiments described below for polymerized material were not performed on samples of the monomer due to the spontaneous polymerization of the monomer when exposed to room or laser light, X-ray radiation, or the electron beam as observed in other polydiacetylenes.[38]

Characterization of the polymerized blue solid by X-ray diffraction (Figure 3) clearly demonstrates its highly crystalline nature and its spontaneous macroscopic orientation over the length scale of a centimeter. The X-ray scans reveal 14 orders of (00l) reflections, indicating the sample is an exceedingly ordered layered assembly of macromolecules with a layer normal perpendicular to the plane of the film. The X-ray scans in

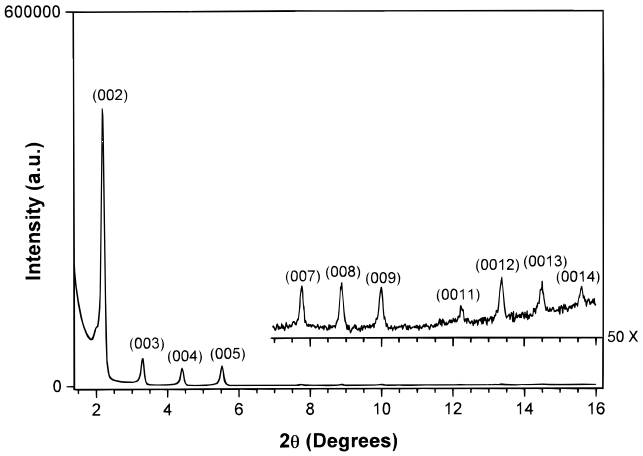

Figure 3. Room temperature wide angle X-ray diffraction scan revealing the high degree of long-range order in the layered two-dimensional supramolecular structure. The inset shows a magnification of 50 of the *y*-axis revealing up to the 14th order (00l) reflection at 15.6°.

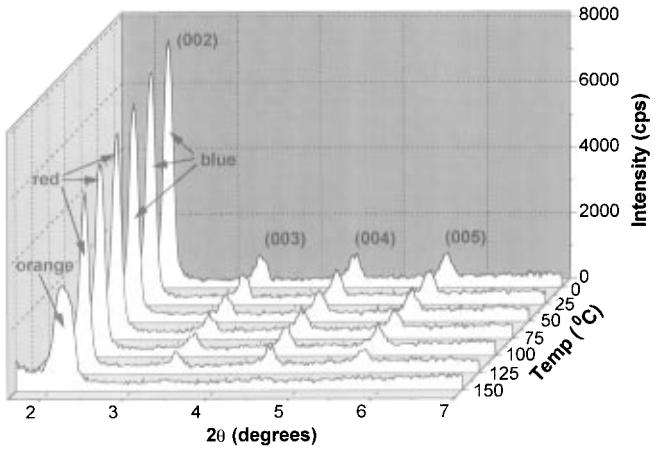

Figure 4. Variable temperature wide angle X-ray scan revealing disordering of the lattice between 125 and 150 °C.

Figure 4 indicate that long-range order deteriorates with rising temperature although the material remains birefringent. The *d* spacing of the (002) peak increases by 1.41 Å from 39.20 Å at 0 °C to 40.61 Å at 150 °C. Within the range 125−150 °C, a change occurs from a well-ordered to a less-ordered state as indicated by the broadening of the (002) peak and the disappearance of higher order peaks with rising temperature. This broadening of the (002) peak also corresponds to the gradual red to orange chromic change observed in this solid. Changes in morphology in this temperature range have been studied by Li and Stupp.[39]

The nature of hydrogen bonding was characterized by variable temperature Fourier transform infrared spectroscopy. It is known that sharp OH stretching bands associated with dimeric hydrogen bonding are observed in the range 3550−3450 cm^{-1}, and broad bands typical of polymeric hydrogen bonding are observed in the range 3400−3200 cm^{-1}.[40] The observed peak maximum for our material in KBr pellet form appears at 3300 cm^{-1} (see Figure 5). This indicates that hydroxyl groups at the side chain terminus, R_2 (see Figure 11), engage in polymeric rather than dimeric hydrogen-bonding. The FTIR experiment shows a loss in absorption for the polymeric hydrogen bonding peak with increasing temperature. Spectra obtained at different temperatures in the wavenumber range 3555−3020 cm^{-1} are shown in Figure 6. IR absorption in this

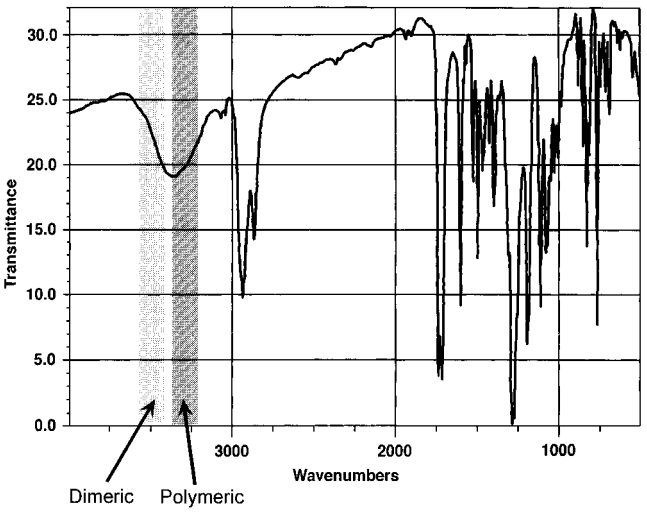

Figure 5. Room temperature FTIR spectrum of the material in KBr pellet form. The ranges for dimeric and polymeric hydrogen bonding are shown at 3550−3450 and 3400−3200 cm^{-1}, respectively.

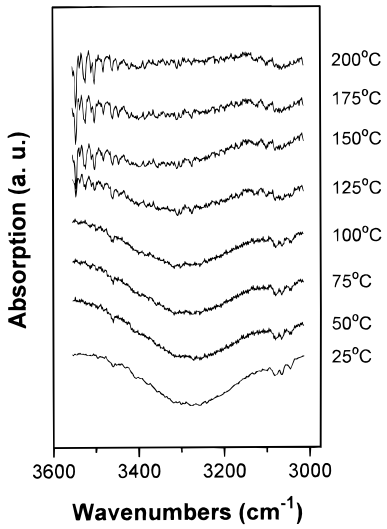

Figure 6. Variable temperature FTIR spectra of the 2D material cast on a single-crystalline silicon substrate (sample rotation with respect to incident radiation = 55°).

range disappears entirely between 175 and 200 °C. Upon cooling the sample from 200 °C to room temperature, the hydrogen bonding reappears, although the peak lacks some of its original intensity. This could be related to structural changes linked to the irreversible red to orange thermochromic transition when samples are heated above 110 °C. This is shown clearly in Figure 7 in a plot of normalized peak area as a function of temperature, determined from Gaussian fits of the spectra. Interestingly, however, the center of the fitted peak shifts to higher energy as temperature is increased (Figure 8) from 3277 to 3320 cm^{-1}. We were unable to fit the spectra obtained at 200 °C. As temperature is increased, we expect next-nearest neighbor interactions to decrease and nearest neighbor bonds to dominate, this leading to a trend toward dimeric as opposed to polymeric hydrogen bonding. The increase in force constant for OH stretching results in a change of 43 cm^{-1} for the absorption maximum as the sample is heated from 25 to 175 °C (3277−3320 cm^{-1}). This is nearly reversible upon cooling, with $\nu_{46°C}$ 3292 cm^{-1}, deviating by only 4.6 cm^{-1} from the expected value of 3287 cm^{-1}, assuming a linear increase in ν upon heating between 25 and 50 °C. We believe "polymeric" hydrogen

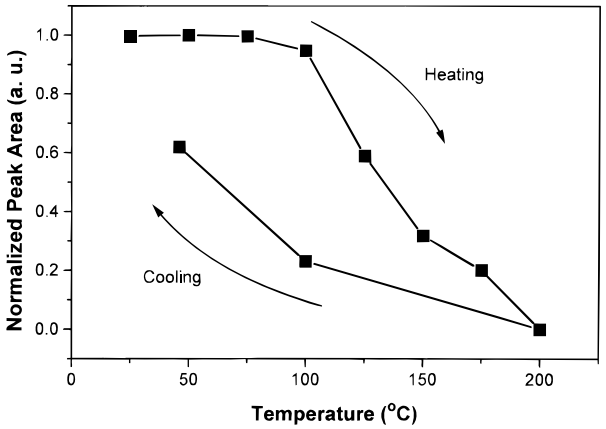

Figure 7. Plot of normalized peak area of Gaussian fits versus temperature showing the loss of hydrogen bonding with temperature and the partial irreversibility upon cooling.

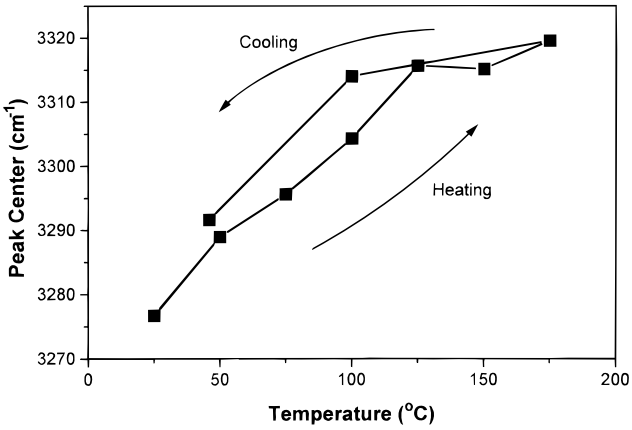

Figure 8. Plot of the peak center versus temperature showing the nearly reversible shift to higher energy from 3277 to 3320 cm^{-1}.

bonding in this system, fingerprinted by the very broad IR bands observed, is the factor that provides two-dimensional cohesion to the self-assembled structure. This cohesion would not exist in the structure if only dimeric hydrogen bonds were to prevail in the form of intramolecular bonds among polydiacetylene chains or between two comb chains. The total density of hydrogen bonds does not appear to be reversible as evident in Figure 7. This probably is the result of irreversible morphological changes which occur when the material is heated to very high temperatures. These changes are discussed in another publication from our laboratory.[39]

We observed a correlation between the thermochromic transitions and the DSC endotherms and exotherms. The blue to red thermochromic transition around 62 °C is clearly evident in Figure 9. The endotherm seen in the first heating is accompanied by an exotherm on cooling and is observed again in the second heating, demonstrating the reversibility of the blue to red thermochromic transition. In contrast, the irreversible nature of the physical process which causes the red to orange thermochromic transition is suggested by the DSC scan shown in Figure 10. Once the material is heated above 145 °C and the solid becomes orange in color, the first endotherm is no longer observed. However, three other transitions are observed by DSC above this temperature which remain reversible (see Figure 10). The origin of the endotherm observed during the blue to red transition remains unclear since lattice parameters remain unchanged.[39]

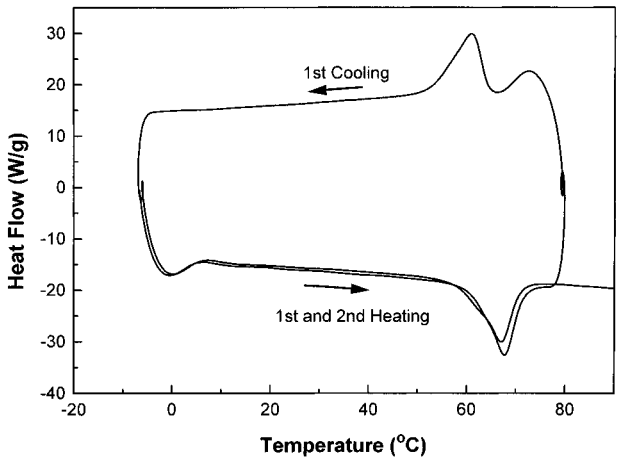

Figure 9. DSC scans showing the reversibility of a transition which coincides with the chromic change from blue to red.

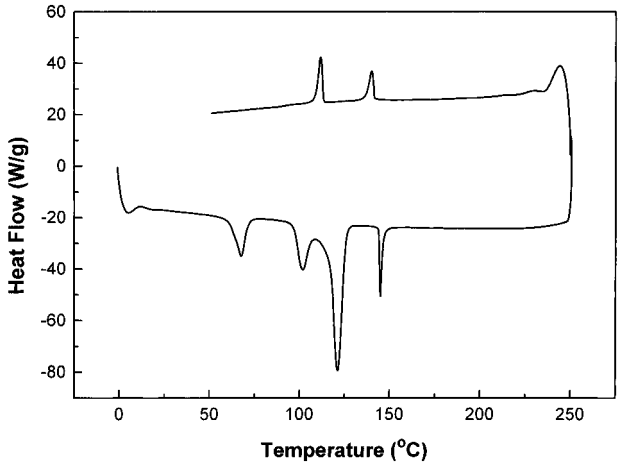

Figure 10. DSC scans showing the irreversibility of the 62 °C transition once the material is heated above 120 °C.

As mentioned earlier, hydrogen bonding among the polydiacetylene backbones can lead to either ladder or two-dimensional structures. The polymeric hydrogen bonding observed can result in the formation of either ladders or two-dimensional objects depending on the direction of hydrogen bonding relative to the direction of covalent backbones. However, the broad peak observed indicates that nonequidistant OH groups, nearest neighbors, and next-nearest neighbors are interacting, and therefore both intra- and interladder hydrogen bonding must be occurring in the system. This should result in the formation of a multidirectional hydrogen-bonded plane between unidirectional backbones. This delocalized hydrogen-bonded plane binds polydiacetylene chains in the nearest upper and lower backbone-containing planes that form the two-dimensional bilayer structure depicted in Figure 11. Thus, we believe the polymerization of the diacetylene compound results in a 2D supramolecular structure as a result of polymeric hydrogen bonding.

As the blue solid is heated, a strong linear chromic change occurs as is typical of many polydiacetylenes.[1,41,42] At 25 °C the first absorption maximum occurs at 630 nm (1.972 eV) (see Figure 12). This peak blue shifts with temperature: the largest shift in the absorption maximum (53 nm) occurs between 25 and 50 °C while the material changes chromically to the eye from blue to bright red. Another large change in the peak maximum as a function of temperature occurs between 125 and 150 °C which coincides with the endotherm observed by DSC at 145 °C.

Nonlinear Optical Properties. The third-order susceptibility coefficient was obtained using optical band gap data from UV−vis−near infrared spectra and also sum frequency generation experiments. The linear chromic data of the absorption peak obtained from UV−vis−near infrared can be used to predict the third-order nonlinear optical properties of the material and compared with values obtained from sum frequency generation. Calculations of cubic hyperpolarizabilities of polyenes and polydiacetylenes can be calculated in the framework of a one-dimensional sinusoidal pseudopotential as initially performed by Ducuing et al.[43,44] and later improved upon for infinite polymeric chains by Sauteret et al.[45] The band gap susceptibility, $\chi_{zzzz}^{(3)}$, which gives a rough estimate of the NLO properties is given by the following expression:

$$\chi_{zzzz}^{(3)} = \frac{2^5\pi^2 e^{10}}{45\sigma}\left(\frac{a_o}{d}\right)^3 \frac{1}{E_g^{\,6}} \qquad (1)$$

where energy E_g is the band gap energy, a_o is the Bohr radius = 0.5292 Å,[46] d is the average carbon−carbon bond distance, and σ is the cross-sectional area per chain. From electron diffraction data, $d = 1.21$ Å and $\sigma = 187 \times 10^{-16}$ cm^2.[39] Inserting the E_g values obtained from variable temperature UV−vis−near infrared spectra yields the values of $\chi_{zzzz}^{(3)}$ plotted in Figure 13. The largest change in $\chi_{zzzz}^{(3)}$ occurs between 25 °C, 2.06×10^{-11} esu and 50 °C, 1.29×10^{-11} esu, corresponding to the large thermochromic transition of the solid from blue to red. An increase in temperature results in a gradual decrease in $\chi_{zzzz}^{(3)}$, to 0.96×10^{-11} esu at 125 °C. Corresponding to the bright red to orange thermochromic transition, $\chi_{zzzz}^{(3)}$ experiences a larger decrease to 0.74×10^{-11} esu at 150 °C, and finally the $\chi_{zzzz}^{(3)}$ levels off between 150 and 200 °C. Comparing the trend of the optical band gap data with that obtained by sum frequency generation yields interesting results. Although the absolute values of the band gap and the sum frequency data do not coincide in Figure 13, the third-order susceptibility calculated from absorption data predicts an abrupt and large 37% decrease in $\chi_{zzzz}^{(3)}$ at the blue to red chromic change. This large decrease is not observed in sum frequency generation experiments, where $\chi_{SumFreq}^{(3)}$ decreases by only 7% from 0.90×10^{-11} esu at 20 °C and 0.84×10^{-11} esu at 70 °C. The value of $\chi_{SumFreq}^{(3)}$ seems reasonable due to the large cross-sectional area per chain because of the large side group, R_2. A larger but gradual decrease is observed between 70 and 110 °C followed by a modest and irreversible decrease to 3×10^{-12} esu as a temperature of 200 °C is approached. $\chi_{SumFreq}^{(3)}$ then remains constant at 3×10^{-12} esu while the sample is cooled to room temperature and then reheated to 200 °C. Thus, the large change in $\chi^{(3)}$ calculated from band gap measurements as the blue to red thermochromic transition occurs is not observed experimentally. Equation 1 applies to isolated chains, but intermolecular interactions between the closely packed chains (4.0 Å[39]) may play a role in stabilizing third-order nonlinear optical properties or in the observed thermochromic transition. As discussed in the following paper of this issue, morphological changes occur over the experimental temperature range which disrupt the 2D structure. These changes could also play a role in the observed chromic changes.

Interestingly, our material exhibits excellent photochemical stability when exposed to the intense Nd:YAG

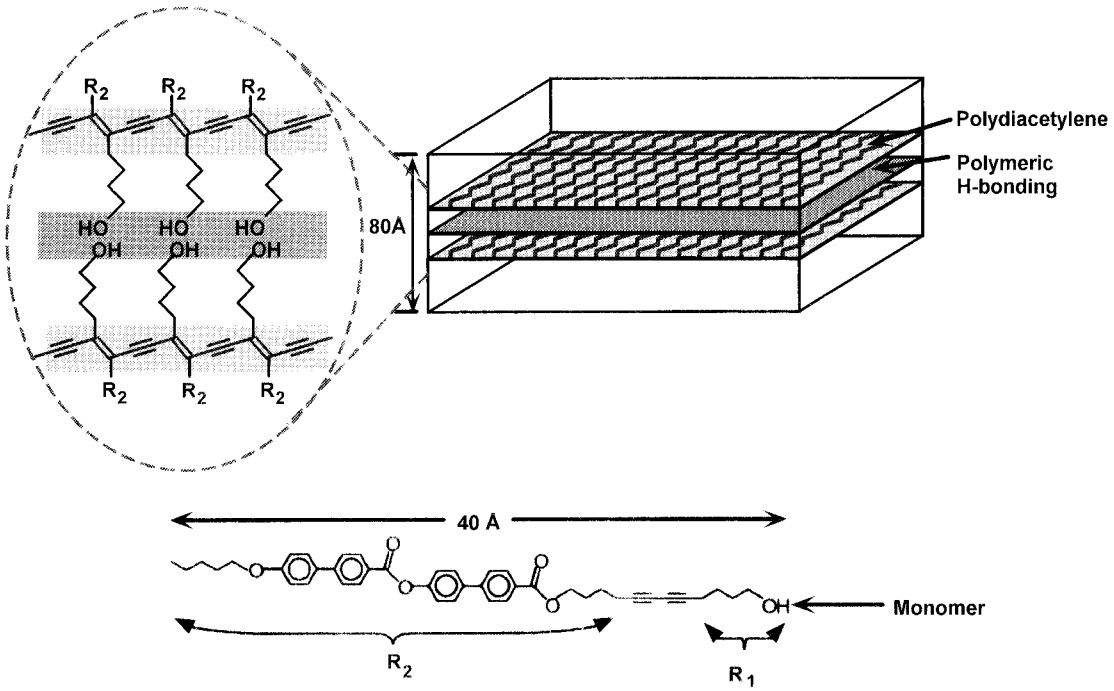

Figure 11. Schematic representation of a bilayer supramolecular object formed by covalent and hydrogen bonds. Covalent bonds are represented by the coplanar black parallel lines, and the dotted plane represents a diffuse hydrogen-bonded network that "stitches" together the comb polymers forming the bilayer.

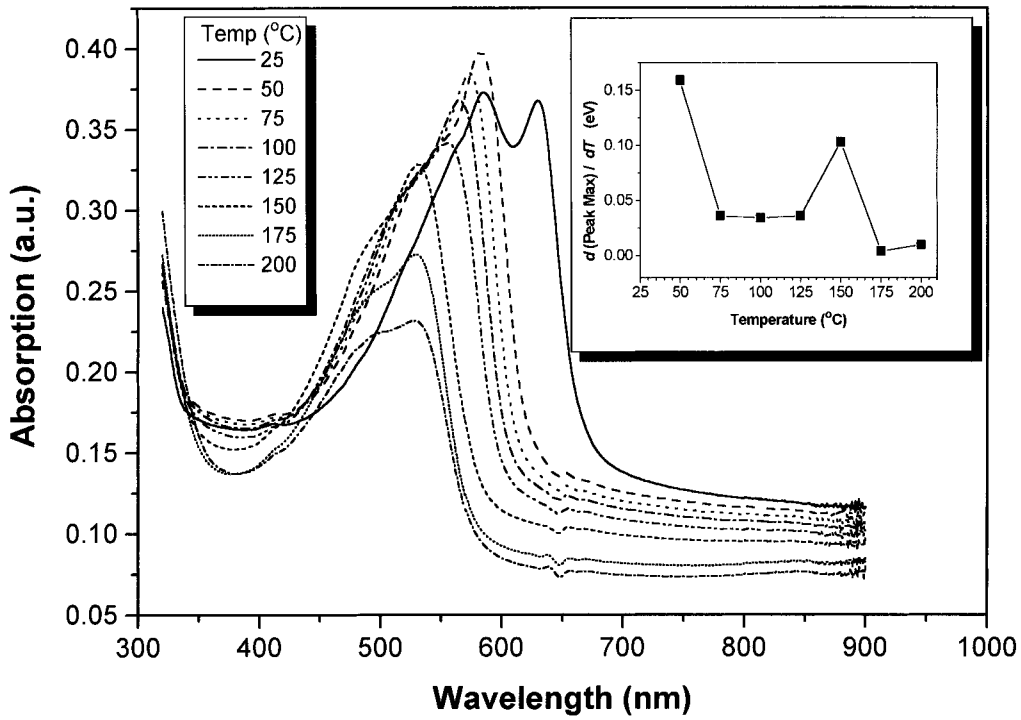

Figure 12. UV−vis−near infrared spectra showing the peak absorption of polymerized crystalline material. The inset shows the change in the peak maximum with temperature. Note that the greatest shifts occur between 25 and 50 °C and between 125 and 150 °C.

laser radiation required to measure third-order susceptibility. The material does not show any evidence of damage after being irradiated by nearly 0.5 million pulses of 28 MW/cm^2 peak intensity light. This stability was not observed in another polymer prepared from a hairpin-shaped derivative of molecule **5**[47] with less conjugation in its polydiacetylene backbones and possibly an architecture with lower two dimensionality than the structure studied here. The hairpin-derived polymer was thermally more stable (decomposing at 346 °C) than the hydrogen-bonded 2D structure resulting from polymerization of **5** (decomposed at 300 °C). However, the hairpin-derived polymer as well as the 1D linear polymer poly(phenylenevinylene) burned when exposed to much lower intensities of the laser beam relative to the hydrogen-bonded 2D structure (<10 MW/cm^2). While absorption of the infrared beam can explain the difference in photochemical stability of the various materials, some of the stability in the structure derived from molecule **5** could result from the ability of the highly ordered 2D assemblies to dissipate the energy of phonons from IR absorption.

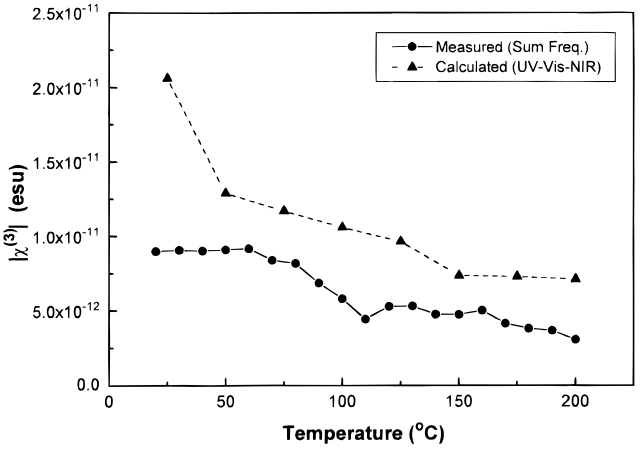

Figure 13. Calculated values of $|\chi_{zzzz}^{(3)}|$ from optical absorption measurements as a function of temperature and measured values using sum frequency generation experiments as a function of temperature, $|\chi_{SumFreq}^{(3)}(-3\omega;\omega,\omega,\omega)|$.

Conclusions

A diacetylene molecule was reported that polymerizes to form a highly ordered two-dimensional supramolecular structure through a network of polymeric hydrogen bonding. This structure exhibits significant photochemical stability when exposed to laser radiation, and this property may be connected to its two-dimensional architecture. Intermolecular interactions in these highly ordered structures may play a role in thermochromic changes and third-order nonlinear optical properties.

Acknowledgment. The authors are grateful to the U.S. Department of Energy, Office of Basic Energy Sciences, for funding this work through Grant DEFG02-96ER45439, obtained through the Materials Research Laboratory (MRL) of the University of Illinois. We are also grateful to Doug Wake and Ray Strange of the MRL Laser facility for their invaluable technical assistance with NLO experiments.

References and Notes

(1) Hayden, L. M.; Kovel, S. T.; Srinivasan, M. P. *Opt. Commun.* **1987**, *61*, 351.
(2) Day, D.; Hub, H.-H.; Ringsdorf, H. *Isr. J. Chem.* **1979**, *18*, 325.
(3) Asakuma, S.; Okada, H.; Kunitake, T. *J. Am. Chem. Soc.* **1988**, *113*, 1749.
(4) Kim, T.; Crooks, R. M.; Tsen, M.; Sun, L. *J. Am. Chem. Soc.* **1995**, *117*, 3963.
(5) Batchelder, D. N.; Evans, S. D.; Freeman, T. L.; Häussling, L.; Ringsdorf, H.; Wolf, H. *J. Am. Chem. Soc.* **1994**, *116*, 1050.
(6) Rehage, H.; Schnabel, E.; Vessié, M. *Makromol. Chem.* **1988**, *189*, 2395.
(7) Sakata, K.; Kunitake, T. *Chem. Lett.* **1989**, 2159.
(8) Asakuma, S.; Okada, H.; Kunitake, T. *J. Am. Chem. Soc.* **1991**, *113*, 1749.
(9) Stupp, S. I.; Son, S.; Lin, H. C.; Li, L. S. *Science* **1993**, *259*, 59.
(10) Bolger, J.; Harvery, T. G.; Ji, W.; Kar, A. K.; Molyneux, S.; Wherrett, B. S.; Bloor, D.; Norman, P. *J. Opt. Soc. Am. B* **1992**, *9* (9), 1552.
(11) Carter, G. M.; Thakur, M. K.; Chen, Y. J.; Hryniewicz, J. V. *Appl. Phys. Lett.* **1985**, *47* (5), 457.
(12) Craig, G. S. W.; Cohen, R. E.; Schrock, R. R.; Esser, A.; Schrof, W. *Macromolecules* **1995**, *28*, 2512.
(13) McBranch, D.; Sinclair, M.; Heeger, A. J.; Patil, A. O.; Shi, S.; Askari, S.; Wudl, F. *Synth. Met.* **1989**, *29*, E85.
(14) Jenekhe, S. A.; Roberts, M.; Agrawal, A. K.; Meth, J. S.; Vanherzeele, H. In *Optical and Electrical Properties of Polymers*; Emerson, J. A., Torkelson, J. M., Eds.; MRS: Boston, 1990; Vol. 214, p 55.
(15) Kim, W. H.; Jiang, X. L.; Kumar, J.; Tripathy, S. K. *Pure Appl. Chem.* **1995**, *67* (12), 2023.
(16) Berkovic, G.; Shen, Y. R.; Prasad, P. N. *J. Chem. Phys.* **1987**, *87* (3), 1897.
(17) Meredith, G. R.; Buchalter, B.; Hanzlik, C. *J. Chem. Phys.* **1983**, *78* (3), 1533.
(18) Meredith, G. R.; Buchalter, B.; Hanzlik, C. *J. Chem. Phys.* **1983**, *78* (3), 1543.
(19) Thalhammer, M.; Penzkofer, A. *Appl. Phys. B* **1983**, *32*, 137.
(20) Kajzar, F.; Messier, J. In *Nonlinear Optical Properties of Organic Molecules and Crystals*; Chemla, D. S., Zyss, J., Eds.; Academic: Orlando, 1987; Vol. 2, p 51.
(21) Bosshard, C.; Spreiter, R.; Gunter, P.; Tykwinski, R. R.; Schreiber, M.; Diederich, F. *Adv. Mater.* **1996**, *8*, 231.
(22) Wegner, G. *Makromol. Chem.* **1972**, *154*, 35.
(23) Schott, M.; Wegner, G. In *Nonlinear Optical Properties of Organic Molecules and Crystals*; Chemla, D. S., Zyss, J., Eds.; Academic: Orlando, 1987; Vol. 2, p 3.
(24) Peachy, N. M.; Eckhardt, C. J. *J. Phys. Chem.* **1994**, *98*, 7106.
(25) Baughman, R. H. *J. Appl. Phys.* **1972**, *43*, 4362.
(26) Melveger, A. J.; Baughman, R. H. *J. Polym. Sci.: Polym. Phys. Ed.* **1973**, *11*, 603.
(27) Stupp, S. I.; Son, S.; Li, L. S.; Lin, H. C.; Keser, M. *J. Am. Chem. Soc.* **1995**, *117*, 5212.
(28) Tanaka, H.; Gomez, M. A.; Tonelli, A. E.; Lovinger, A. J.; Davis, D. D.; Thakur, M. *Macromolecules* **1989**, *22*, 2427.
(29) Wang, W.; Lieser, G.; Wegner, G. *Liq. Cryst.* **1993**, *15*, 1.
(30) Moore, J. S.; Stupp, S. I. *Macromolecules* **1990**, *23*, 65.
(31) Gray, G. W.; Hartley, J. B.; Jones, B. *J. Chem. Soc.* **1955**, *236*, 1412.
(32) Heflin, J. R.; Cai, Y. M.; Garito, A. F. *J. Opt. Soc. Am. B* **1991**, *8*, 2132.
(33) Tanaka, H.; Gomez, M. A.; Tonelli, A. E.; Thakur, M. *Macromolecules* **1989**, *22*, 1208.
(34) Wenz, G.; Müller, M. A.; Schmidt, M.; Wegner, G. *Macromolecules* **1984**, *17*, 837.
(35) Nava, A. D.; Thakur, M.; Tonelli, A. E. *Macromolecules* **1990**, *23*, 3055.
(36) Shand, M. L.; Chance, R. R.; LePostollec, M.; Schott, M. *Phys. Rev. B* **1982,** *25*, 4431.
(37) Huggins, K. E.; Stork, K. F.; Son, S.; Bohn, P. W.; Stupp, S. I. *APS Bull.* **1995**, *40* (1), 158.
(38) Batchelder, D. N.; Evans, S. D.; Freeman, T. L.; Häussling, L.; Ringsdorf, H.; Wolf, H. *J. Am. Chem. Soc.* **1994**, *116*, 1050.
(39) Li, L. S.; Stupp, S. I. *Macromolecules* **1997**, *30*, 5313.
(40) Rao, C. N. R. *Chemical Application of Infrared Spectroscopy*; Academic: New York, 1963.
(41) Exarhos, G. J.; Risen, W. M., Jr.; Baughman, R. H. *J. Am. Chem. Soc.* **1976**, *98*, 481.
(42) Tanaka, H.; Thakur, M.; Gomez, M. A.; Tonelli, A. E. *Polymer* **1991**, *32*, 1834.
(43) Rustagi, K. C.; Ducuing, J. *Opt. Commun.* **1974**, *10*, 258.
(44) Ducuing, J. In *Nonlinear Spectroscopy*; Bloembergen, N., Ed.; North-Holland: Amersterdam, 1977; p 276.
(45) Sauteret, C.; Hermann, J.-P.; Frey, R.; Pradère, F.; Ducuing, J.; Baughman, R. H.; Chance, R. R. *Phys. Rev. Lett.* **1976**, *36*, 956.
(46) *CRC Handbook of Chemistry and Physics*, 76th ed.; Lide, D. R., Ed.; CRC Press: Boca Raton, FL, 1995; pp 1−2.
(47) Son, S. Ph.D. Thesis, University of Illinois, 1994.

MA961715I